

MIT Open Access Articles

Large-scale quantum photonic circuits in silicon

The MIT Faculty has made this article openly available. **Please share** how this access benefits you. Your story matters.

Citation: Harris, Nicholas C. et al. "Large-Scale Quantum Photonic Circuits in Silicon." Nanophotonics 5.3 (2016): n. pag.

As Published: <http://dx.doi.org/10.1515/nanoph-2015-0146>

Publisher: Walter de Gruyter

Persistent URL: <http://hdl.handle.net/1721.1/107670>

Version: Final published version: final published article, as it appeared in a journal, conference proceedings, or other formally published context

Terms of use: Creative Commons Attribution-NonCommercial-NoDerivs License



Review article

Open Access

Nicholas C. Harris, Darius Bunandar, Mihir Pant, Greg R. Steinbrecher, Jacob Mower, Mihika Prabhu, Tom Baehr-Jones, Michael Hochberg and Dirk Englund*

Large-scale quantum photonic circuits in silicon

DOI 10.1515/nanoph-2015-0146

Received November 25, 2015; revised March 8, 2016; accepted March 8, 2016

Abstract: Quantum information science offers inherently more powerful methods for communication, computation, and precision measurement that take advantage of quantum superposition and entanglement. In recent years, theoretical and experimental advances in quantum computing and simulation with photons have spurred great interest in developing large photonic entangled states that challenge today's classical computers. As experiments have increased in complexity, there has been an increasing need to transition bulk optics experiments to integrated photonics platforms to control more spatial modes with higher fidelity and phase stability. The silicon-on-insulator (SOI) nanophotonics platform offers new possibilities for quantum optics, including the integration of bright, nonclassical light sources, based on the large third-order nonlinearity ($\chi^{(3)}$) of silicon, alongside quantum state manipulation circuits with thousands of optical elements, all on a single phase-stable chip. How large do these photonic systems need to be? Recent theoretical work on Boson Sampling suggests that even the problem of sampling from ~ 30 identical photons, having passed through an interferometer of hundreds of modes, becomes challenging for classical computers. While experiments of this size are still challenging, the SOI platform has the required component density to enable

low-loss and programmable interferometers for manipulating hundreds of spatial modes.

Here, we discuss the SOI nanophotonics platform for quantum photonic circuits with hundreds-to-thousands of optical elements and the associated challenges. We compare SOI to competing technologies in terms of requirements for quantum optical systems. We review recent results on large-scale quantum state evolution circuits and strategies for realizing high-fidelity heralded gates with imperfect, practical systems. Next, we review recent results on silicon photonics-based photon-pair sources and device architectures, and we discuss a path towards large-scale source integration. Finally, we review monolithic integration strategies for single-photon detectors and their essential role in on-chip feed forward operations.

Keywords: quantum; optics; photonics; silicon; linear optics.

1 Introduction

Photons can encode quantum states, and various approaches for universal quantum computation have been proposed that rely on some forms of interactions between these photons. For photons in integrated waveguide circuits, a sufficiently strong interaction may be possible using nonlinearities of single atom-like systems [1–7]. Photon loss and mode distortion [8, 9] can cause gate errors, but heralded gates [10] may help. Alternatively, it was shown by Knill et al. [11] that an effective nonlinear interaction between single photons can be produced by the act of measurement, enabling heralded probabilistic logic gates that can be sufficient, in principle, for fault-tolerant quantum computing by using teleportation and feed-forward. This result motivated more efficient theoretical proposals [12–15] for linear optical quantum computing and related linear optics experiments [16, 17]. Large entangled states may be produced without the demanding feed-forward operations using the percolation approach

*Corresponding author: Dirk Englund, Department of Electrical Engineering and Computer Science, Massachusetts Institute of Technology, 77 Massachusetts Avenue, Cambridge, MA 02139, USA, e-mail: englund@mit.edu

Nicholas C. Harris, Mihir Pant, Greg R. Steinbrecher, Jacob Mower and Mihika Prabhu: Department of Electrical Engineering and Computer Science, Massachusetts Institute of Technology, 77 Massachusetts Avenue, Cambridge, MA 02139, USA

Darius Bunandar: Department of Physics, Massachusetts Institute of Technology, 77 Massachusetts Avenue, Cambridge, MA 02139, USA

Tom Baehr-Jones and Michael Hochberg: Coriant Advanced Technology, 171 Madison Avenue, Suite 1100, New York, NY 10016, USA

[18], though feed-forward is still necessary in the subsequent cluster state quantum computation [19]. As Boson Sampling [20, 21] does not feed-forward or error correction, it promises a near-term win of a quantum system over classical machines [22], but still requires hundreds of spatial modes [23–26]. Scaling up these approaches, it is necessary to develop photonic systems with hundreds of phase-stable, low-loss, coupled optical modes along with a method for generating many indistinguishable single photons [24, 27]. Because of the need for phase stability between large numbers of spatial modes, chip-integrated approaches are likely necessary [28–30].

Much progress has been made using low index contrast integrated waveguide technologies, such as planar, laser-written silica-on-silicon waveguides, with mode field dimensions similar to those of single-mode optical fibers. Demonstrations include two-photon quantum simulations [31], boson sampling [25, 26, 32–34] in circuits with between 5 and 13 waveguide modes, and up to four photons in each separate mode post-selected controlled-NOT (CNOT) gates [16, 33], quantum teleportation [35] with probabilistic Bell state measurement, and bosonic quantum walks [36] of two photons. Since index contrast determines the size of optical components – for example, through the minimum bending radius enabling total internal reflection – waveguide technologies with higher index contrast are needed to scale to higher component densities.

Nanophotonics in the silicon-on-insulator (SOI) waveguide platform exhibits high index contrast, enabling bend radii down to $2\ \mu\text{m}$ [37], and therefore dramatically reduced component dimensions. In addition, silicon has a large third-order nonlinear coefficient ($\chi^{(3)}$) for implementing photon-pair sources [38–43] and an extensive set of electrically active and passive photonic devices. Recent work has also demonstrated the integration of highly efficient single-photon detectors with silicon quantum photonic circuits [44, 45].

2 Silicon nanophotonics for quantum optics

Silicon photonics benefits from strong backing from industry and academia. This is at least partly due to its compatibility with the fabrication tools, techniques, and test equipment developed by the semiconductor electronics industry and optical fiber telecommunications industry [46]. In addition, silicon photonics fabrication services have become available [47], enabling fabless development of photonic integrated circuits. Recently,

silicon nanophotonics has been used for quantum optical experiments [38, 41–44, 48–50] – an application with unique fabrication and design challenges. As summarized in Figure 1, quantum optics applications require low bending loss, propagation loss, waveguide cross-talk, and photoluminescence.

A typical SOI process stack is shown in Figure 1A with a silicon waveguiding layer ($n_1=3.5$ at 1550 nm) between two glass (SiO_2) layers ($n_2=1.54$ at 1550 nm), resulting in a high index contrast of 40%, as outlined in Table 1, and subsequently large component densities. High index contrast, coupled with low-loss fabrication processes, enables compact optical components with waveguide bend radii down to $2\ \mu\text{m}$ [37]. SOI nanophotonics platforms have been used to implement systems containing hundreds of optical components on a single chip [48, 57, 58].

The probability of an N -photon coincidence decreases exponentially with normalized transmission probability; therefore, reducing photon loss is critical. In SOI, propagation losses as low as 0.3 dB/cm [51, 59] have been achieved at a wavelength of 1550 nm – a value that is similar to competing photonics technologies outlined in Table 1. Reducing photon loss is an essential requirement in linear optics quantum applications, since error correction of nonheralded photon losses is extremely challenging [27]. Improved fabrication processes, such as surface oxidation [53], may enable further reductions in photon loss.

3 Large-scale linear optical circuits

To date, the majority of integrated quantum optical experiments have been performed using waveguide circuits that effectively constitute N -port interferometer circuits that perform unitary transformations on N spatial modes. Reck et al. [60] showed that any element of the $U(N)$ group can be decomposed into a succession of $N(N-1)/2$ individual $U(2)$ elements. If each of these $U(2)$ elements is implemented by an electrically tunable Mach-Zehnder interferometer with at least two phase shifters – a reconfigurable beamsplitter (RBS) as shown in Figure 2A – then the entire $U(N)$ transformation can be implemented in a fully reconfigurable way, as shown in Figure 2B. The first such circuits to program arbitrary single-photon unitary transformations were recently demonstrated [33, 48]. Besides applications for quantum information processing, recent proposals have investigated classical applications of such circuits [61, 62].

The RBS can be realized using two 50% reflectivity beamsplitters with adjustable internal and external phase

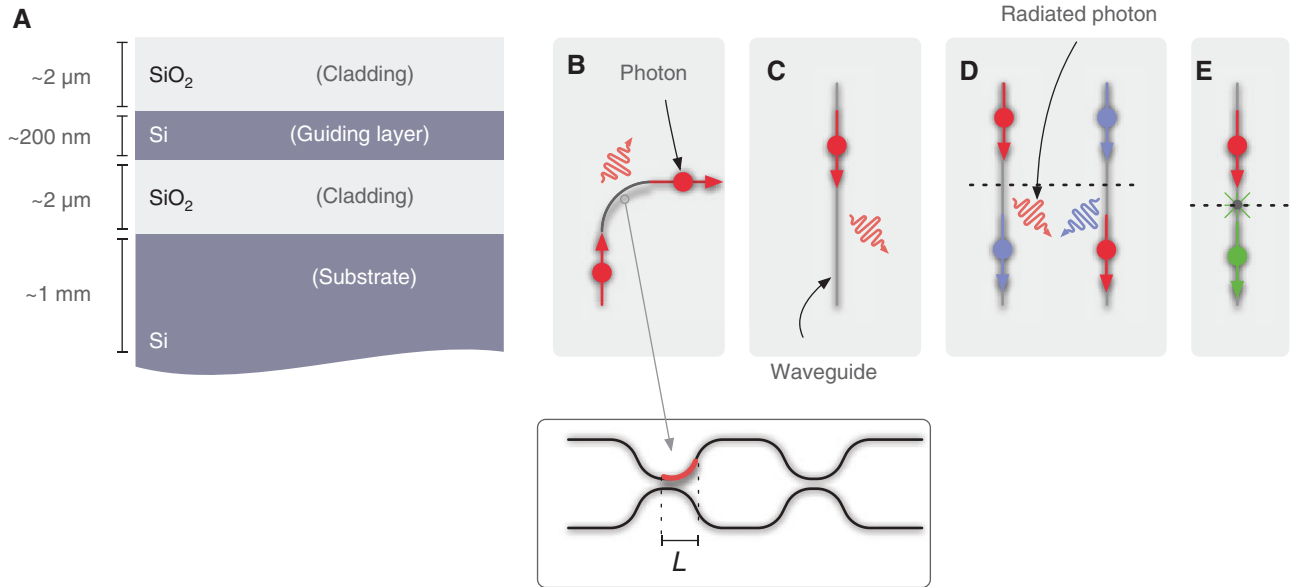


Figure 1: Quantum photonics in the SOI platform. (A) Silicon-on-insulator process stack with a thick silicon substrate layer and SiO_2 cladding a silicon guiding layer. Typical layer dimensions are shown. (B) Schematic depiction of waveguide bend and inset showing an interferometer incorporating many waveguide bends of length L . Waveguide bend radius fundamentally depends on index contrast and limits the number of optical elements integrable on a single photonic chip. (C) Schematic diagram of lossy scattering from a silicon waveguide. Quantum photonic circuits are highly sensitive to propagation loss since it results in an exponential reduction in multiphoton coincidence probability – limiting the ability to perform multiphoton experiments. (D) Depiction of cross-talk between waveguides modes. Cross-talk between components results in lower success probabilities for quantum operations. (E) Schematic depiction of absorption and reemission process in silicon. Silicon exhibits low photoluminescence due to its indirect band gap, which requires multiphoton absorption events for 1550 nm excitation or phonon-assisted transitions.

Table 1: Summary of integrated photonics platform parameters.

Material system	λ	Photoluminescence	Loss (dB/cm)	Δn (%)	Fabrication complexity
SOI	Near IR	Indirect	2.4–0.3 [51, 52]	40	Low
Silica-on-silicon	Near IR	–	0.1 [5]	0.5	Low
Si_3N_4	Visible, near IR	Yes	1.5 [53]/ 5×10^{-4} [54]	18	Medium
LiNbO_3	Near IR	No data	10–0.6 [55]	29	High
InP	Near IR	No data	>2 [56]	Varies	Medium

Index contrast is calculated as $\Delta n = (n_{\text{core}}^2 - n_{\text{clad}}^2) / (2n_{\text{core}}^2)$ and serves as a predictor for optical component density. IR, infrared.

shifters and is described by the linear-optical Bogoliubov transformation:

$$U_{\text{RBS}} = \begin{bmatrix} e^{i\Phi} \sin(\Theta) & e^{i\Phi} \cos(\Theta) \\ \cos(\Theta) & -\sin(\Theta) \end{bmatrix}, \quad (1)$$

where Φ is the phase differential between the two external arms of the Mach-Zender Interferometer and Θ is the phase differential between the two internal arms. The external phases of RBSs in consecutive layers can be combined into one differential phase δ , thereby enabling any rotation in $SU(2)$.

The ability to generate arbitrary linear-optical circuits in the spatial-mode basis comes at the cost of control

complexity. For example, an arbitrary $U(20)$ transformation would require 190 RBS unit cells, each with two electronically controlled phase shifters, totaling 380 electrical connections. The electrical control circuitry of this magnitude typically requires the design of custom control systems [33, 48].

Figure 3A shows a programmable quantum photonic processor (QPP) fabricated in the OpSIS silicon nanophotonics foundry [52]. The QPP consists of a mesh of 56 electrically tunable RBS unit cells with an average measured visibility of 0.9993 ± 0.0002 [48] and an on-chip loss of <2 dB, excluding the one-time, off-chip coupling losses. The majority of on-chip loss is attributed to a waveguide propagation loss of 2.4 dB/cm [52]. Each RBS unit cell, shown in Figure

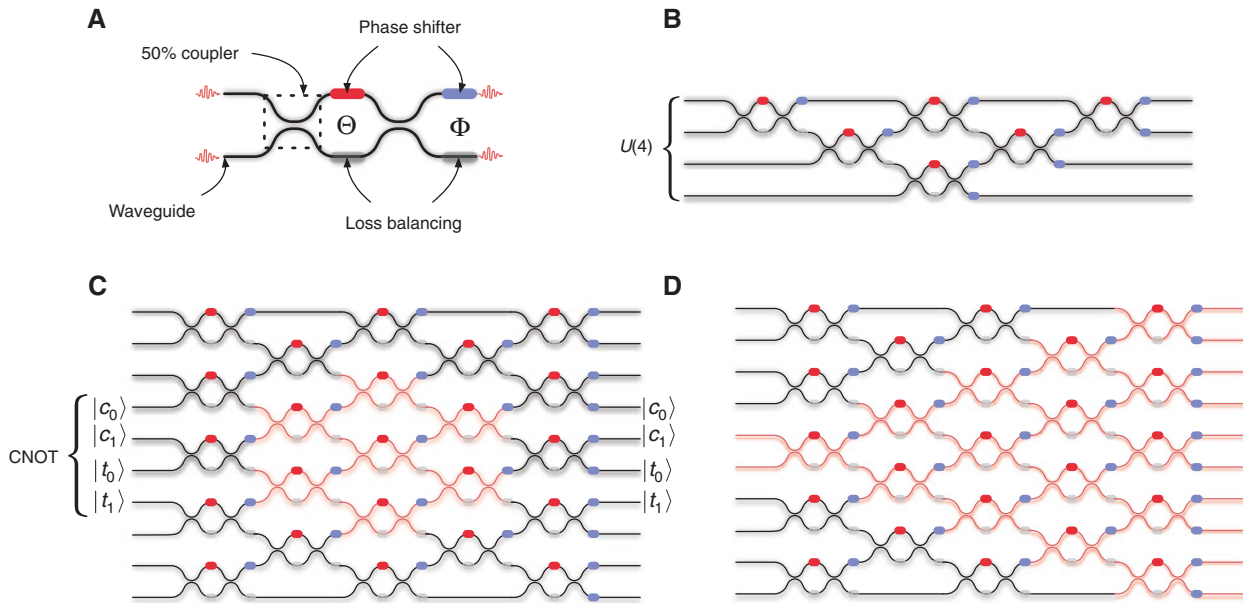


Figure 2: A programmable photonic circuit. (A) RBS unit cell. (B) Mesh of RBS unit cells implementing an arbitrary four-dimensional, single-particle unitary transformation. (C) Footprint for an embedded postselected CNOT gate with control and target modes labeled as $|c_{0,1}\rangle$ and $|t_{0,1}\rangle$, respectively [28]. (D) Footprint of circuit for exploring quantum transport phenomena [49].

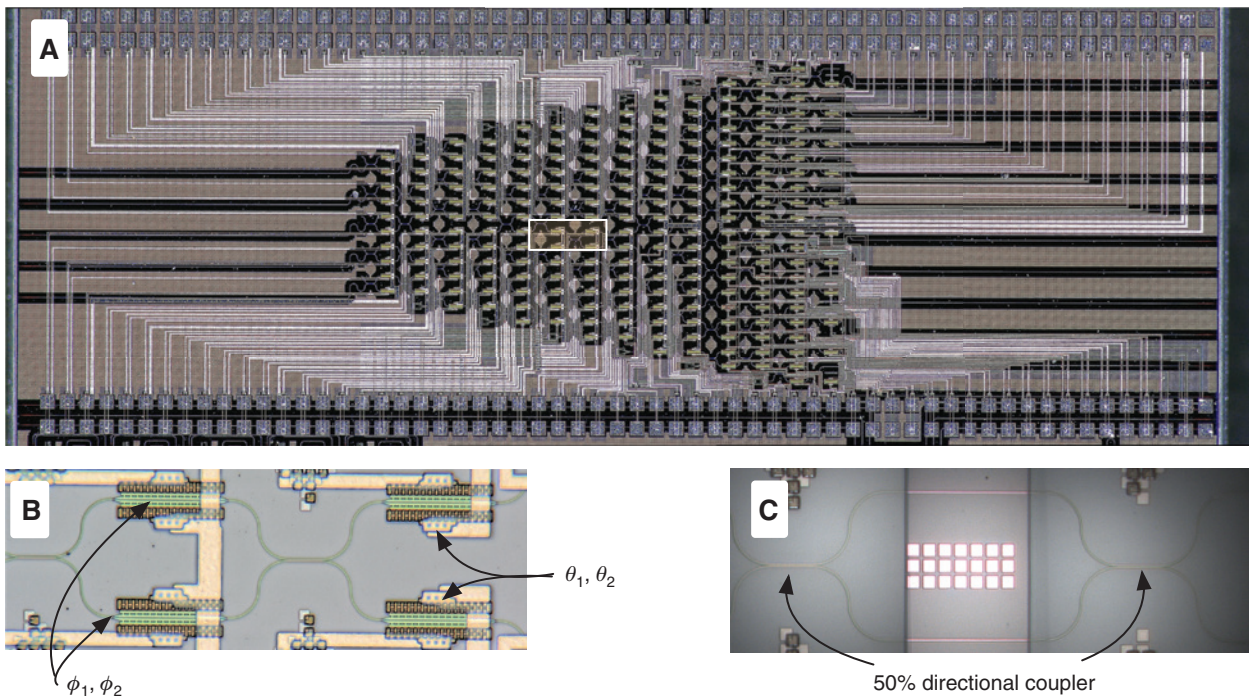


Figure 3: Optical micrographs of QPP fabricated in a silicon photonics platform. (A) The QPP measures 4.9 mm by 1.7 mm and is composed of 56 Mach-Zehnder interferometers, 213 phase shifters, and 112 directional couplers. The average RBS visibility was measured to be 0.9993 ± 0.0002 . (B) Single RBS unit cell with two internal and two external low-loss phase shifters. (C) RBS unit cell test structure without phase shifters. Waveguides and directional couplers are shown.

3B and C, contains four thermo-optic phase shifters [63] and two 50:50 splitting ratio directional couplers. The QPP phases can be programmed on microsecond timescales [63]. High-speed phase modulators are available in the silicon

photonics platform with switching rates of tens of gigahertz [64], although insertion losses limit their usage for quantum optics. The fast reconfigurability of this circuit enables experiments that explore many different phase settings,

such as modeling of quantum transport phenomena [48]. Using a reconfigurable silica circuit with six modes, Carolan et al. [33] recently demonstrated boson sampling with a six-photon state. Generalized quantum photonic circuits such as this silicon-based circuit, or silica-based circuits [33], may shorten the time between theoretical conception and experimental realization for a wide range of quantum photonic protocols, including boson sampling, gate model quantum computing, and quantum simulation.

Practical integrated photonic RBS unit cells suffer from nonidealities due to variations in the splitting ratio of the 50% reflectivity beamsplitter, propagation losses associated with phase shifting elements and waveguide imperfections and imbalances that can reduce interferometric visibility.

Fixed-reflectivity beamsplitters in integrated photonic platforms can be implemented by nearly lossless evanescent mode coupling between nearby waveguides [65]. Evanescent mode couplers are inherently dispersive, with a power splitting ratio that varies as $\sin^2(\pi L \Delta n / \lambda_0)$, where Δn is the effective index difference between the super mode between the two waveguides and a single waveguide mode, L is the adjacency length, and λ_0 is the free space wavelength. Variation in the ideally 50% reflectivity beamsplitters limits the interferometric visibility of the RBS unit cell and the precision with which it can implement certain two-mode transforms including direct routing or swapping the input.

In silicon, phase modulation is achieved using either plasma dispersion [66] or the relatively strong thermo-optic effect; strained silicon can also exhibit an electro-optic effect [67]. Plasma dispersion modulators can reach speeds of several tens of gigahertz [60, 68]. Unfortunately, plasma dispersion is an inherently lossy phase modulation mechanism since a change in the refractive index caused by a free-carrier concentration change also results in a change in absorption [69]. While thermal time constants in SOI are generally in the microsecond range, small temperature changes produce large phase shifts ($dn/dt = 1.86 \cdot 10^{-4} K^{-1}$ [59]) – enabling low-loss phase shifters measuring just a few tens of microns [59, 70].

Small phase differences caused by waveguide edge-wall roughness are accumulated throughout an interferometer mesh, resulting in an initially unknown unitary evolution. Recent theoretical work has considered the problem of characterizing such systems using single- and two-photon interference [48, 56, 71, 72]. While the exponential reduction in multiphoton coincidence rates associated with uniform loss cannot be corrected post fabrication, the operational fidelity of a quantum circuit program in the QPP architecture can be greatly improved using nonlinear

optimization techniques [68]. Figure 4A–D shows 1000 (300) instances of CNOT [16] (controlled-phase [CPHASE] [17]) gates programmed into nonideal QPPs. Before nonlinear optimization (shown in light gray in Figure 4A and C), the average CNOT (CPHASE) gate fidelity was 94.52% (92.22%). After optimization, average gate fidelities (shown in dark grey in Figure 4A and C) of 99.99% were achieved for both CNOT and CPHASE gates.

4 Single-photon and multiphoton sources

4.1 Spontaneous four-wave mixing in silicon

Indistinguishable photons are an essential resource for many photonic quantum information processing protocols [73]. A range of phenomena enabling single-photon and multiphoton generation are being developed, including parametric processes in nonlinear crystals and on-demand single-photon sources based on semiconductor quantum dots. The former photon generation process is stochastic, yet readily available in standard integrated photonics material systems; the latter process can be near-deterministic, but challenges remain with regards to large-scale integration.

Silicon has a large third-order nonlinearity ($\chi^{(3)}$) that enables photon-pair generation by spontaneous four-wave mixing (SFWM), as outlined in Figure 5A–C. SFWM can be used as either a stochastic source of entangled photon pairs or a heralded source of single photons.

Mathematically, SFWM is described via the following nonlinear Hamiltonian,

$$H_{NL} \propto \hat{a}_p^2 \hat{a}_i^\dagger \hat{a}_s^\dagger + h.c. \quad (2)$$

where $\hat{a}_p, \hat{a}_s^\dagger, \hat{a}_i^\dagger$ are the pump field annihilation operator and signal and idler creation operators, respectively. The Hermitian conjugate ($h.c.$) term describes the reverse process. These processes conserve both energy and momentum, satisfying $2\omega_p = \omega_s + \omega_i$, as shown in Figure 5A, and $2k_p = k_s + k_i$ (phase-matching). Due to the squared dependence of the SFWM process on the pump field intensity [74], much work has focused on developing field-enhancing photonic structures.

4.2 Photonic structures

Demonstrations of structures that enhance photon generation rates via SFWM include rectangular waveguides

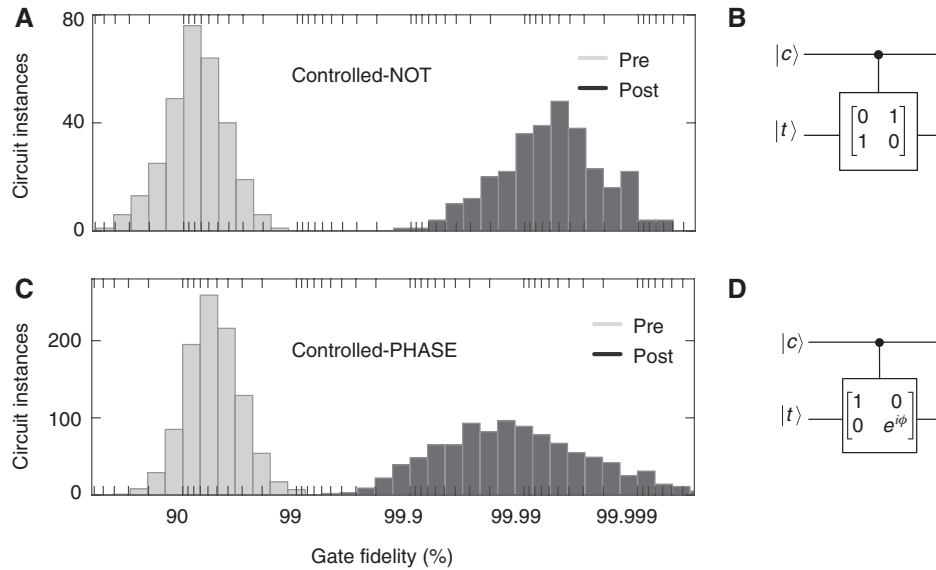


Figure 4: Improving postselected CNOT and CPHASE gate fidelities with a nonlinear optimization algorithm. (A) Performance of the CNOT gate program in a realistic simulation of the QPP architecture. Light and dark grey histograms plot fidelity before and after optimization of phase settings. (B) The CNOT gate flips the state of a target qubit $|t\rangle$ if and only if a control qubit $|c\rangle$ is present. (C) Preoptimization and postoptimization results for the CPHASE gate program within simulated QPPs. In each simulation, reported fidelities are the minimum over six different choices of the phase applied by the controlled operation, equally distributed from 0 to 2π . (D) The CPHASE gate applies a phase shift to a target qubit $|t\rangle$ if and only if a control qubit $|c\rangle$ is present.

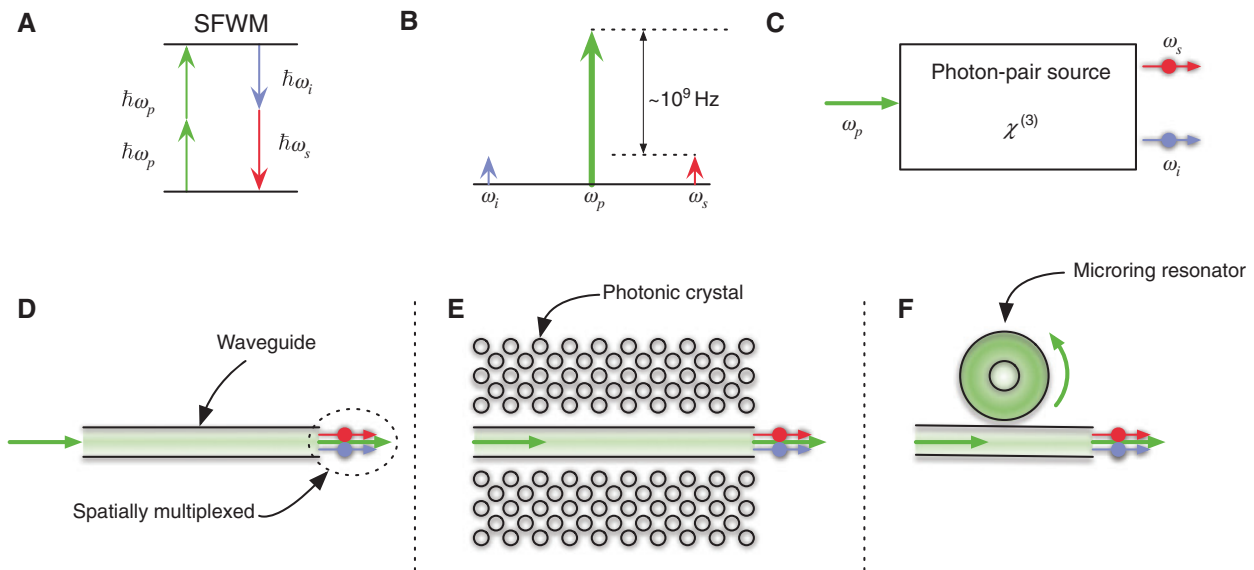


Figure 5: Integrated SFWM structures. (A) SFWM process. Two photons of energy $\hbar\omega_p$ are annihilated, creating a pair of quantum-correlated photons of energies $\hbar\omega_s$ and $\hbar\omega_i$, respectively. (B) Schematic comparison of photon-pair intensity to the pump field, which is typically a factor of 10^9 higher intensity. (C) Ideal model of a photon-pair source based on SFWM. A pump field is incident on a $\chi^{(3)}$ nonlinear crystal; the photon pair at the output is spatially demultiplexed and the pump field is not present. (D–F) Integrated SFWM structures used to enhance the pump intensity, resulting in a higher photon-pair output flux for a given input pump flux with respect to bulk-optical implementations. (E) A slow-light photonic crystal structure with a high group index increases the nonlinear interaction time, giving rise to a higher output flux intensity. (F) A microring resonator structure integrates the pump field, resulting in a higher output flux intensity.

[42, 49, 75, 76], slow-light photonic crystal structures [50, 77–79], and microring resonators [38, 41, 43, 80–88]; see Figure 5D–F. As SFWM involves the annihilation of two photons, pair generation rates scale with the square of the optical intensity. With standard single-mode waveguide geometries of 500 nm by 220 nm, optical intensities in integrated structures are enhanced by the inverse of the effective mode area [70] with respect to bulk-silicon SFWM pair sources.

In slow-light photonic crystal SFWM sources, shown in Figure 5E, the pump field group velocity $v_g = c/n_g$ is reduced with respect to the bulk phase velocity $v_0 = c/n_0$. Photon-pair generation rates in these structures scale as S^4 , where $S = n_g/n_0$ is the slow-down factor [50, 89, 90], with one factor of S^2 associated with an increased accumulated nonlinear phase shift and another factor of S^2 resulting from spatial compression of the electromagnetic field.

In microring resonator-based SFWM sources, shown in Figure 5F, the pump field is evanescently coupled into a cavity formed by a waveguide loop, or ring. The cavity supports a set of resonances spaced by $\Delta\lambda = \lambda_0^2 / (2\pi r n_g)$, where λ_0 is the center wavelength and r is the ring radius. Pair generation rates are enhanced as Q^3/R^2 , where Q is the quality factor of the microring resonator and R is the ring radius [38, 43, 80, 91].

4.3 Photon-pair sources for large-scale systems

To allow SFWM sources to be integrated with detectors, the pump light needs to be filtered on-chip. This is challenging, as the pump field intensity is typically 100 dB or more above the signal and idler field intensities. Experimental demonstrations of SFWM photon-pair sources have relied on the use of bulk-optical components for pump field filtering – an approach that becomes challenging for large numbers of photon-pair sources both due to off-chip coupling losses and implementation complexity. Recent work has taken steps toward addressing these challenges, demonstrating 95 dB of pump field isolation on-chip [38].

Figure 6 shows a SFWM circuit fabricated in a complementary metal-oxide semiconductor (CMOS)-compatible silicon photonics process [38, 58]. The operation of the circuit is schematically shown in Figure 6B. The pump field is coupled onto the chip using grating couplers and subsequently routed to a critically coupled, electrically tunable microring resonator with a loaded Q of $\approx 40,000$, where signal and idler photons are

generated. The pump field, which has been attenuated by the pair-generation ring extinction ratio, and photon pairs then pass through a distributed Bragg reflector, which rejects the pump wavelength by 65 dB. Finally, the signal and idler photons are demultiplexed using thermo-optically tunable microring resonators acting as add-drop filters, which further attenuate the pump below that of the signal and idler fields, as illustrated in Figure 6B. Internal pair generation rates of 10 MHz with a coincidence-to-accidental ratio of 50 were achieved – limited by two-photon absorption in silicon, which can be mitigated using carrier-depletion techniques [92]. Isolation of unguided pump light from out-coupling ports is challenging and can be a limiting factor in achieving pump extinction ratios exceeding 100 dB. In the experiments reported in Ref. [38], photon pairs were generated on chip and then transferred to a second chip using single-mode, polarization maintaining optical fibers, which included another distributed Bragg reflector resulting in a total pump isolation of more than 150 dB.

Approaching the ideal SFWM photon-pair source “black-box” in Figure 5C with complete pump filtering, spatial de-multiplexing of photon pairs, and high pair-brightness is within the reach of current integrated photonics technologies. Further, the nondeterminism of SFWM-based single-photon sources may be improved through the use of temporal-multiplexing schemes. In such schemes, one of two photons generated by a photon-pair source is sent to a single-photon detector – heralding the temporal position of the other photon. By using a switch and photon storage element, such as a fiber delay line or an optical cavity, the remaining photon can be multiplexed onto a targeted time window – increasing the probability of finding a photon in a desired time bin. There have been a number of theoretical proposals [93, 94] and recent experimental demonstrations [95–98] of temporal multiplexing. In addition to temporal-multiplexing schemes, spatial-multiplexing schemes have been proposed [99, 100] and demonstrated [50, 101] in order to reduce the probability of multipair emission events, which reduce the determinism of χ^2 - and χ^3 -based single-photon sources.

5 Single photon detection

Single-photon detection at 1550 nm has been performed using off-chip InGaAs single-photon avalanche detectors, superconducting nanowire single-photon detectors (SNSPDs), and superconducting transition edge sensors [102]. Off-chip detection has several downsides, including

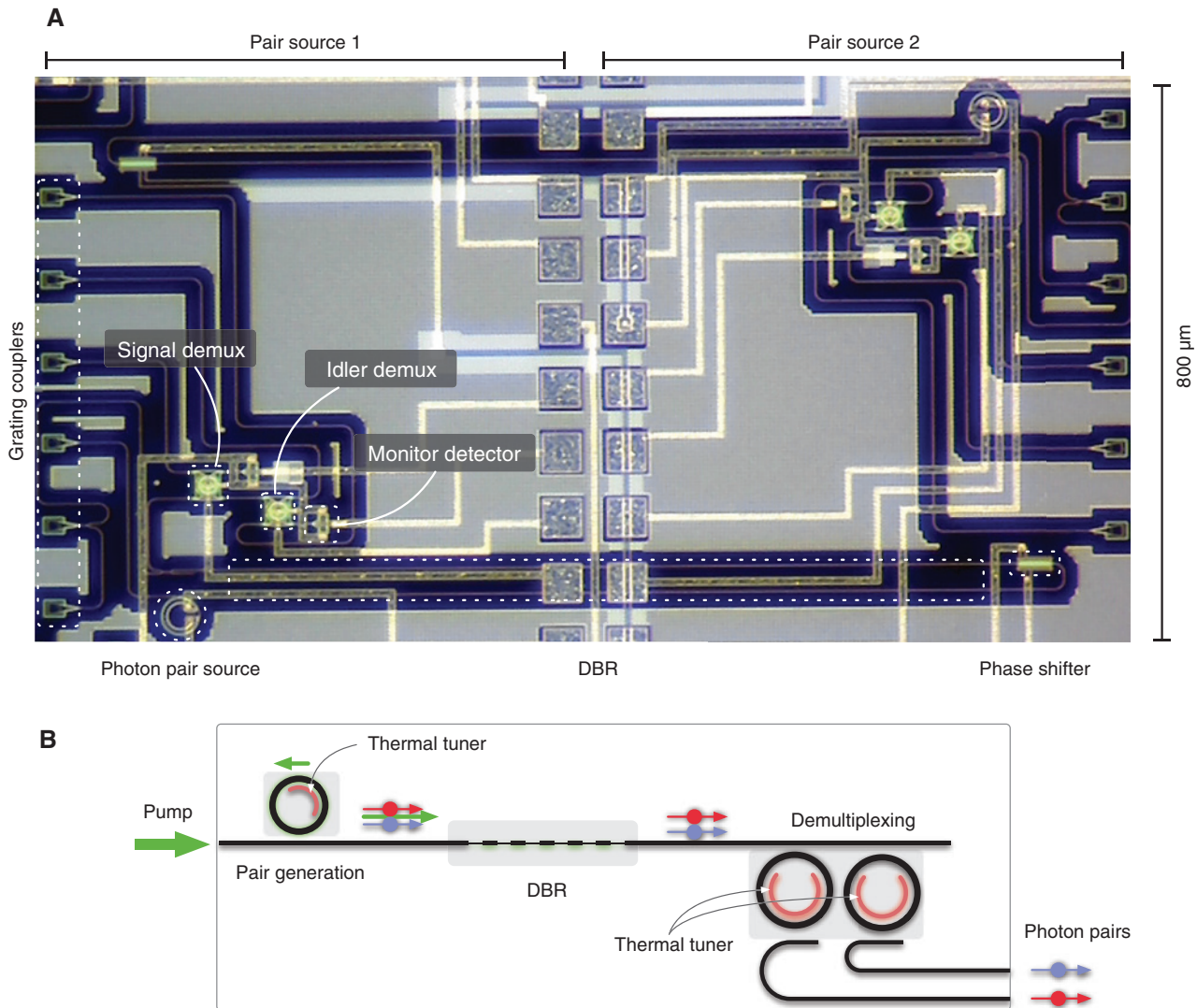


Figure 6: Optical micrograph of integrated photon-pair sources fabricated in a silicon photonics platform. (A) Optical micrograph of chip containing two photon-pair sources. (B) Schematic representation of the system depicted in the micrograph in (A). A pump field excites a microring resonator, generating pairs of quantum-correlated photons. The generated pairs and pump field pass through a distributed Bragg reflector (DBR), where the pump field is suppressed. Finally, the signal and idler photons are spatially demultiplexed using two microring resonators resonant with the signal and idler wavelengths λ_s and λ_i , respectively.

loss associated with coupling out of a chip (an effective detection efficiency reduction), electronic delay, and wiring complexity. Monolithic integration of single-photon detectors with integrated photonic circuits containing electro-optically active components could enable feed-forward by reconfiguring optical paths in response to the detection of one or more photons, as required for scalable linear optics quantum computing.

Among single-photon detection technologies, SNSPDs are particularly attractive. Recent experimental work on tungsten silicide SNSPDs has shown 90% detection efficiencies [103]. In the niobium nitride material system, SNSPDs with jitter below 30 ps [104] and count

rates in the gigahertz range [105] have been shown. However, the integration of multiple high-efficiency SNSPDs into integrated photonics platforms has proven challenging [106, 107]. Low system yield has prompted new strategies for integrating SNSPDs into photonic circuits, including micrometer-scale flip-chip techniques, in which only high-performance SNSPDs are selected for integration onto photonic circuits, resulting in a yield improvement.

Figure 7 shows SOI circuits with many integrated niobium nitride SNSPDs and outlines the micron-scale flip-chip process [44]. Each SNSPD shown was evaluated in a cryostat and selected for high performance

before being integrated with a quantum photonic circuit. This technique was used to assemble a proof-of-concept system with two input ports coupled to 50:50 beamsplitters with a detector on each of the output ports – enabling the first on-chip second-order correlation function $g^{(2)}(\tau)$ measurements. The inputs were excited with photon pairs generated by an off-chip spontaneous parametric down-conversion source, revealing photon-bunching in the on-chip detection statistics. In the same paper, a silicon quantum photonic circuit with 10 niobium nitride SNSPDs, each with sub-50 ps jitter, was demonstrated (see Figure 7).

6 Outlook

Photonic quantum technologies have progressed rapidly in recent years. Recent studies on resource requirements of scalable linear optics quantum computing [27] and all-optical quantum repeaters [108] suggest that these

systems will require a large number of photonic elements. While new protocols for the efficient generation of cluster states based on percolation theory [18, 109, 110] may reduce these resource requirements and the number of feed-forward elements, large unitary transformations on many optical modes will still be necessary. Even in boson sampling, recent predictions indicate a crossover to the postclassical computing regime for between $n=20$ and 30 photons populating $m \gg n$ modes [24–26].

Compact, low loss, and gigahertz-rate modulators remain an elusive building block for linear optics quantum computing; they are at the center of proposals for realizing error tolerant quantum photonic circuits [27, 108]. In silicon, lossless modulation at high speed is particularly challenging, since high-speed modulation is achieved using the inherently lossy plasma dispersion effect [62]. Additional scaling of these systems may require low-loss coupling to large numbers of waveguides and the integration of many high-efficiency single photon detectors. Experimental demonstrations of large unitary evolution circuits [33, 48], chip-to-chip

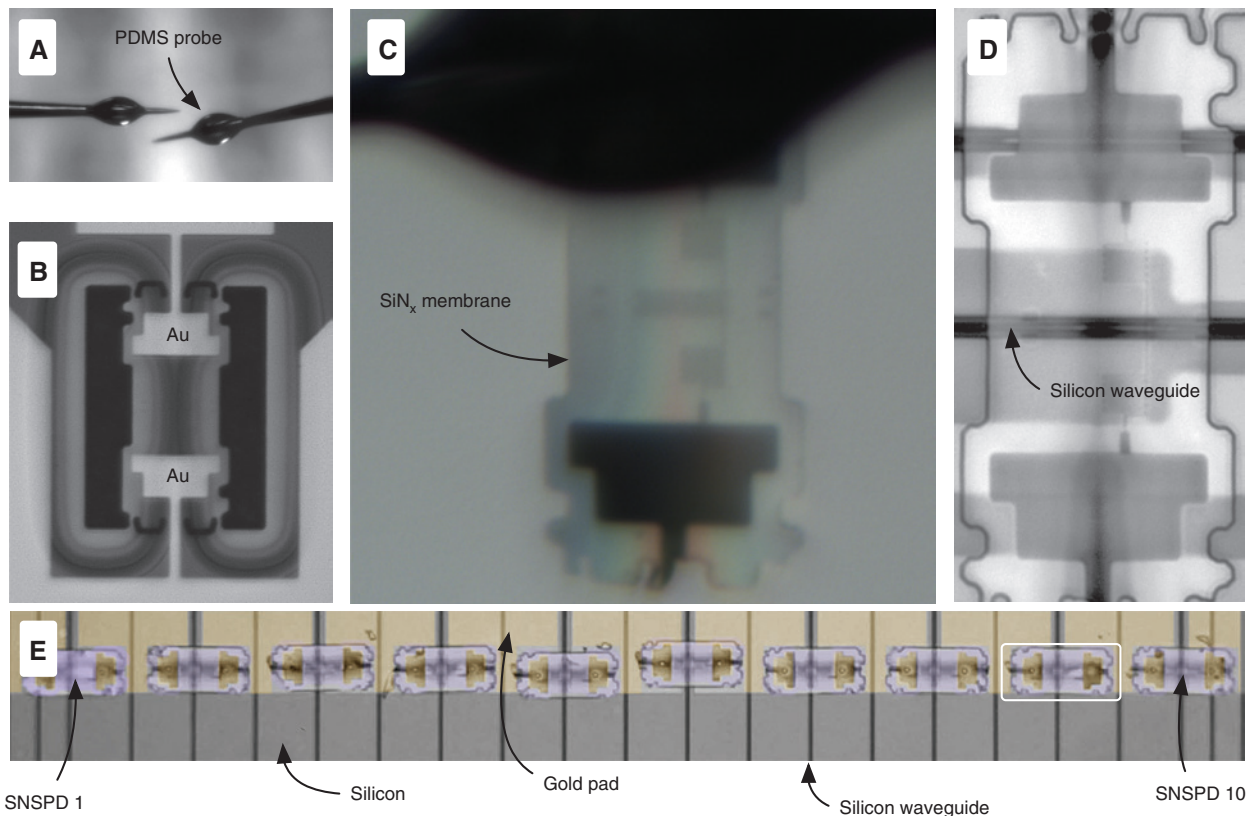


Figure 7: Micro-flip-chip integration of niobium nitride superconducting nanowire single-photon detectors. (A) Polydimethylsiloxane (PDMS) coated tungsten probes used to remove membrane SNSPDs from a silicon nitride substrate shown in (B). (C) SNSPD after being removed from the silicon nitride substrate. (D) SNSPD aligned and placed on a silicon photonic waveguide. (E) Ten SNSPDs aligned and placed on a silicon photonic waveguide array.

quantum state transfer [38, 49], fast all-optical switching [111], and the integration of many SNSPDs on a single silicon chip [44], along with recent theoretical proposals for more resource-efficient linear optical quantum computing [18, 110], may soon enable the demonstration of large-scale linear quantum optics circuits that are hard to simulate on classical computers.

Acknowledgments: This work was supported in part by the Air Force Office of Scientific Research Multidisciplinary University Research Initiative (FA9550-14-1-0052) and the Air Force Research Laboratory RITA program (FA8750-14-2-0120). M.H. acknowledges support from AFOSR STTR, grant numbers FA9550-12-C-0079 and FA9550-12-C-0038, and Gernot Pomrenke, of AFOSR, for his support of the OpSIS effort, through both a PECASE award (FA9550-13-1-0027) and funding for OpSIS (FA9550-10-1-0439). N.H. acknowledges support from the National Science Foundation Graduate Research Fellowship (grant no. 1122374). G.R.S. acknowledges support from the Department of Defense National Science and Engineering Graduate Fellowship. We thank Paul Alsing, Michael Fanto, and Greg Howland for helpful discussions.

References

- [1] Fushman I, Englund D, Faraon A, Stoltz N, Petroff P, Vučković J. Controlled phase shifts with a single quantum dot. *Science* 2008;320:769–72.
- [2] Englund D, Faraon A, Fushman I, Stoltz N, Petroff P, Vučković J. Controlling cavity reflectivity with a single quantum dot. *Nature* 2007;450:857–61.
- [3] Bose R, Sridharan D, Kim H, Solomon GS, Waks E. Low-photon-number optical switching with a single quantum dot coupled to a photonic crystal cavity. *Phys Rev L* 2012;108:227402.
- [4] Volz T, Reinhard A, Winger M, Badolato A, Hennessy KJ, Hu EL, Imamoglu A. Ultrafast all-optical switching by single photons. *Nat Photonics* 2012;6:605–9.
- [5] Srinivasan K, Painter O. Linear and nonlinear optical spectroscopy of a strongly coupled microdisk-quantum dot system. *Nature* 2007;450:862–5.
- [6] Tiecke TG, Thompson JD, de Leon NP, Liu LR, Vuletić V, Lukin MD. Nanophotonic quantum phase switch with a single atom. *Nature* 2014;508:241–4.
- [7] Goban A, Hung C-L, Yu S-P, Hood JD, Muniz JA, Lee JH, Martin MJ, McClung AC, Choi KS, Chang DE, Painter O, Kimble HJ. Atom-light interactions in photonic crystals. *Nat Commun* 2014;5:3808.
- [8] Shapiro JH. Single-photon kerr nonlinearities do not help quantum computation. *Phys Rev A* 2006;73:062305.
- [9] Dove J, Chudzicki C, Shapiro JH. Phase-noise limitations on single-photon cross-phase modulation with differing group velocities. *Phys Rev A* 2014;90:062314.
- [10] Borregaard J, Kómár P, Kessler EM, Sørensen AS, Lukin MD. Heralded quantum gates with integrated error detection in optical cavities. *Phys Rev Lett* 2015;114. <http://dx.doi.org/10.1103/PhysRevLett.114.110502>.
- [11] Knill E, Laflamme R, Milburn GJ. A scheme for efficient quantum computation with linear optics. *Nature* 2001;409:46–52.
- [12] Raussendorf R, Briegel HJ. A One-way quantum computer. *Phys Rev L* 2001;86:5188–91.
- [13] Browne DE, Rudolph T. Resource-efficient linear optical quantum computation. *Phys Rev L* 2005;95:010501.
- [14] Kok P, Munro WJ, Nemoto K, Ralph TC, Dowling JP, Milburn GJ. Linear optical quantum computing with photonic qubits. *Rev Mod Phys* 2007;79:135–74.
- [15] Aspuru-Guzik A, Walther P. Photonic quantum simulators. *Nat Phys* 2012;8. <http://dx.doi.org/10.1038/nphys2253>.
- [16] Politi A, Cryan MJ, Rarity JG, Yu S, O’Brien JL. Silica-on-silicon waveguide quantum circuits. *Science* 2008;320:646–9.
- [17] Kieling K, O’Brien JL, Eisert J. On photonic controlled phase gates. *New J Phys* 2010;12:013003.
- [18] Gimeno-Segovia M, Shadbolt P, Browne DE, Rudolph T. From three-photon Greenberger-Horne-Zeilinger states to ballistic universal quantum computation. *Phys Rev Lett* 2015;115:020502.
- [19] Nielsen MA. Optical quantum computation using cluster states. *Phys Rev Lett* 2004;93:040503.
- [20] Aaronson S, Brod DJ. Boson Sampling with lost photons. *Phys Rev A* 2016; 93:012335.
- [21] Rohde PP, Berry DW, Motes KR, Dowling JP. A quantum optics argument for the #P-hardness of a class of multidimensional integrals. *arXiv preprint* 2016; arXiv:1607.04960.
- [22] Huh J, Guerreschi GG, Peropadre B, McClean JR, Aspuru-Guzik A. Boson sampling for molecular vibronic spectra. *Nat Photonics* 2015;9:615–20.
- [23] Gard BT, Motes KR, Olson JP, Rohde PP, Dowling JP. An introduction to boson-sampling. In: Malinovskaya SA, Novikova I, Wall ML, Hazzard KRA, Rey AM, Olave RG, Win AL, Kemp K, Roof SJ, Balik S, eds. *From atomic to mesoscale: The role of quantum coherence in systems of various complexities*. World Scientific Publishing Co. Pte. Ltd., 2015, 167–92. ISBN: 9789814678704.
- [24] Aaronson S, Arkhipov A. The computational complexity of linear optics. *Proceedings of the 43rd Annual ACM Symposium on Theory of Computing—STOC 2011*. 2011. <http://dx.doi.org/10.1145/1993636.1993682>.
- [25] Spring JB, Metcalf BJ, Humphreys PC, Steven Kolthammer W, Jin X-M, Barbieri M, Datta A, Thomas-Peter N, Langford NK, Kundys D, Gates JC, Smith BJ, Smith PGR, Walmsley IA. Boson sampling on a photonic chip. *Science* 2013;339:798–801.
- [26] Broome MA, Fedrizzi A, Rahimi-Keshari S, Dove J, Aaronson S, Ralph TC, White AG. Photonic boson sampling in a tunable circuit. *Science* 2013;339:794–8.
- [27] Li Y, Humphreys PC, Mendoza GJ, Benjamin SC. Resource costs for fault-tolerant linear optical quantum computing. *Phys Rev X* 2015;5:041007.
- [28] Politi A, Matthews J, Thompson M, O’Brien J. Integrated quantum photonics. *IEEE J Select Top Quantum Electron* 2009;15:1673–84.
- [29] Thompson MG, Politi A, Matthews JC, O’Brien JL. Integrated waveguide circuits for optical quantum computing. *IET Circuits Devices Syst* 2011;5:94–102.

- [30] O'Brien JL, Furusawa A, Vučković J. Photonic quantum technologies. *Nat Photonics* 2009;3:687–95.
- [31] Lanyon BP, Whitfield JD, Gillett GG, Goggin ME, Almeida MP, Kassal I, Biamonte JD, Mohseni M, Powell BJ, Barbieri M, Aspuru-Guzik A, White AG. Towards quantum chemistry on a quantum computer. *Nat Chem* 2010;2:106–11.
- [32] Crespi A, Osellame R, Ramponi R, Brod DJ, Galvão EF, Spagnolo N, Vitelli C, Maiorino E, Mataloni P, Sciarrino F. Integrated multimode interferometers with arbitrary designs for photonic boson sampling. *Nat Photonics* 2013;7:545–9.
- [33] Carolan J, Harrold C, Sparrow C, Martín-López E, Russell NJ, Silverstone JW, Shadbolt PJ, Matsuda N, Oguma M, Itoh M, Marshall GD, Thompson MG, Matthews JCF, Hashimoto T, O'Brien JL, Laing A. Universal linear optics. *Science* 2015;349:711–6.
- [34] Tillmann M, Dakic B, Heilmann R, Nolte S, Szameit A, Walther P. Experimental boson sampling. *Nat Photonics* 2013;7:540–4.
- [35] Metcalf BJ, Spring JB, Humphreys PC, Thomas-peter N, Barbieri M, Steven Kolthammer W, Jin X-M, Langford NK, Kundys D, Gates JC, Smith BJ, Smith PGR, Walmsley IA. Quantum teleportation on a photonic chip. *Nat Photonics* 2014;8:770–4.
- [36] Peruzzo A, Lobino M, Matthews JCF, Matsuda N, Politi A, Poullos K, Zhou X-Q, Lahini Y, Ismail N, Wörhoff K, Bromberg Y, Silberberg Y, Thompson MG, O'Brien JL. Quantum walks of correlated photons. *Science* 2010;329:1500–3.
- [37] Watts MR. Adiabatic microring resonators. *Opt Lett* 2010;35:3231–3.
- [38] Harris NC, Grassani D (equal contribution), Simbula A, Pant M, Galli M, Baehr-Jones T, Hochberg M, Englund D, Bajoni D, Galland C. Integrated source of spectrally filtered correlated photons for large-scale quantum photonic systems. *Phys Rev X* 2014;4:041047.
- [39] Azzini S, Grassani D, Strain MJ, Sorel M, Helt LG, Sipe JE, Liscidini M, Galli M, Bajoni D. Ultra-low power generation of twin photons in a compact silicon ring resonator. *Opt Express* 2012;20:23100–7.
- [40] Takesue H, Matsuda N, Kuramochi E, Notomi M. Entangled photons from on-chip slow light. *Sci Rep* 2014;4:3913.
- [41] Grassani D, Azzini S, Liscidini M, Galli M, Strain MJ, Sorel M, Sipe JE, Bajoni D. A micrometer-scale integrated silicon source of time-energy entangled photons. *Optica* 2014;2:88–94.
- [42] Silverstone J, Bonneau D, Ohira K, Suzuki N, Yoshida H, Iizuka N, Ezaki M, Natarajan CM, Tanner MG, Hadfield RH, Zwiller V, Marshall GD, Rarity JG, O'Brien JL, Thompson MG. On-chip quantum interference between silicon photon-pair sources. *Nat Photonics* 2014;8:104–8.
- [43] Silverstone JW, Santagati R, Bonneau D, Strain MJ, Sorel M, O'Brien JL, Thompson MG. Qubit entanglement between ring-resonator photon-pair sources on a silicon chip. *Nat Comms* 2015;6:7948.
- [44] Najafi F, Mower J, Harris N, Bellei F, Dane A, Lee C, Kharel P, Marsili F, Assefa S, Berggren KK, Englund D. On-chip detection of non-classical light by scalable integration of single-photon detectors. *Nat Commun* 2015;6. <http://dx.doi.org/10.1038/ncomms6873>.
- [45] Pernice W, Schuck C, Minaeva O, Li M, Goltsman GN, Sergienko AV, Tang HX. High-speed and high-efficiency travelling wave single-photon detectors embedded in nanophotonic circuits. *Nat Commun* 2012;3:1325.
- [46] Jalali B, Fathpour S. Silicon photonics. *J Lightwave Technol* 2006;24:4600–15.
- [47] Hochberg M, Baehr-Jones T. Towards fabless silicon photonics. *Nat Photonics* 2010;4:492–4.
- [48] Harris NC, Steinbrecher GR, Mower J, Lahini Y, Prabhu M, Baehr-Jones T, Hochberg M, Lloyd S, Englund D. Bosonic transport simulations in a large-scale programmable nanophotonic processor. *arXiv preprint* 2015. [arXiv:1507.03406](https://arxiv.org/abs/1507.03406).
- [49] Wang J, Bonneau D, Villa M, Silverstone JW, Santagati R, Miki S, Yamashita T, Fujiwara M, Sasaki M, Terai H, Tanner MG, Natarajan CM, Hadfield RH, O'Brien JL, Thompson MG. Quantum photonic interconnect. *Optica* 2016;3:407–13.
- [50] Collins M, Xiong C, Rey IH, Vo TD, He J, Shahnia S, Reardon C, Krauss TF, Steel MJ, Clark AS, Eggleton BJ. Integrated spatial multiplexing of heralded single-photon sources. *Nat Commun* 2013;4:2582.
- [51] Cardenas J, Poitras CB, Robinson JT, Preston K, Chen L, Lipson M. Low loss etchless silicon photonic waveguides. *Opt Express* 2009;17:4752.
- [52] Baehr-Jones T, Ding R, Ayazi A, Pinguet T, Streshinsky M, Harris N, Li J, He L, Gould M, Zhang Y, Eu-Jin Lim A, Liow T-Y, Hwee-Gee Teo S, Lo G-Q, Hochberg M. A 25 Gb/s silicon photonics platform. *ArXiv e-prints* 2012. <http://adsabs.harvard.edu/abs/2012arXiv1203.0767B>.
- [53] Wörhoff K, Heideman RG, Leinse A, Hoekman M. TriPLeX: a versatile dielectric photonic platform. *Adv Opt Technol* 2015;4:189–207.
- [54] Melchiorri M, Daldosso N, Sbrana F, Pavesi L, Pucker G, Kompocholis C, Bellutti P, Lui A. Propagation losses of silicon nitride waveguides in the near-infrared range. *Appl Phys Lett* 2005;86:121111.
- [55] Cai L, Wang Y, Hu H. Low-loss waveguides in a single-crystal lithium niobate thin film. *Opt Lett* 2015;40:3013–6.
- [56] Smit M, Leijtens X, Ambrosius H, Bente E, van der Tol J, Smalbrugge B, de Vries T, Geluk E-J, Bolk J, van Veldhoven R, Augustin L, Thijs P, D'Agostino D, Rabbani H, Lawnciczuk K, Stopinski S, Tahvili S, Corradi A, Kleijn E, Dzibrou D, Felicetti M, Bitincka E, Moskalenko V, Zhao J, Santos R, Gilardi G, Yao W, Williams K, Stabile P, Kuindersma P, Pello J, Bhat S, Jiao Y, Heiss D, Roelkens G, Wale M, Firth P, Soares F, Grote N, Schell M, Debregeas H, Achouche M, Gentner J-L, Bakker A, Korthorst T, Gallagher D, Dabbs A, Melloni A, Morichetti F, Melati D, Wonfor A, Penty R, Broeke R, Musk B, Robbins D. An introduction to inp-based generic integration technology. *Semicond Sci Tech* 2014;29:083001.
- [57] Sun J, Timurdogan E, Yaacobi A, Hosseini ES, Watts MR. Large-scale nanophotonic phased array. *Nature* 2013;493:195–9.
- [58] Hochberg M, Galland C, Ding R, Liu Y, Zhang Y, Harris N, Baehr-Jones T. "The role of a fabless silicon photonics industry in the era of quantum engineering," in *Latin America Optics and Photonics Conference*, LM3C-3, Optical Society of America, 2012.
- [59] Nezhad MP, Bondarenko O, Khajavikhan M, Simic A, Fainman Y. Etch-free low loss silicon waveguides using hydrogen silsesquioxane oxidation masks. *Opt Express* 2011;19:18827.
- [60] Reck M, Zeilinger A, Bernstein HJ, Bertani P. Experimental realization of any discrete unitary operator. *Phys Rev Lett* 1994;73:58–61.
- [61] Miller DAB. Perfect optics with imperfect components. *Optica* 2015;2:747–50.

- [62] Miller DAB. Self-configuring universal linear optical component. *Photon Res* 2013;1:1–15.
- [63] Harris NC, Ma Y, Mower J, Baehr-Jones T, Englund D, Hochberg M, Galland C. Efficient, compact and low loss thermo-optic phase shifter in silicon. *Opt Express* 2014;22:10487–93.
- [64] Streshinsky M, Ding R, Liu Y, Novack A, Yang Y, Ma Y, Tu X, Chee EK, Lim AE, Lo PG, Baehr-Jones T, Hochberg M. Low power 50 gb/s silicon traveling wave mach-zehnder modulator near 1300 nm. *Opt Express* 2013;21:30350.
- [65] Mikkelsen JC, Sacher WD, Poon JKS. Dimensional variation tolerant silicon-on-insulator directional couplers. *Opt Express* 2014;22:3145–6.
- [66] Soref R, Bennett B. Electrooptical effects in silicon. *IEEE J Quantum Electron* 1987;23:123–129.
- [67] Jacobsen RS, Andersen KN, Borel PI, Fage-Pedersen J, Frandsen LH, Hansen O, Kristensen M, Lavrinenko AV, Moulin G, Ou H, Peucheret C, Zsigri B, Bjarklev A. Strained silicon as a new electro-optic material. *Nature* 2006;441:199–202.
- [68] Baehr-Jones T, Ding R, Liu Y, Ayazi A, Pinguet T, Harris NC, Streshinsky M, Lee P, Zhang Y, Eu-Jin Lim A, Liow T-Y, Hwee-Gee Teo S, Lo G-Q, Hochberg M. Ultralow drive voltage silicon traveling-wave modulator. *Opt Express* 2012;20:12014–20.
- [69] Reed GT, Mashanovich G, Gardes FY, Thomson DJ. Silicon optical modulators. *Nat Photonics* 2010;4:518–26.
- [70] Watts MR, Sun J, DeRose C, Trotter DC, Young RW, Nielson GN. Adiabatic thermo-optic mach-zehnder switch. *Opt Lett* 2013;38:733–5.
- [71] Dhand I, Khalid A, Lu H, Sanders BC. Accurate and precise characterization of linear optical interferometers. *J Opt* 2016;18:035204.
- [72] Mower J, Harris NC, Steinbrecher GR, Lahini Y, Englund D. High-fidelity quantum state evolution in imperfect photonic integrated circuits. *Phys Rev A* 2015;92:032322.
- [73] Migdall A, Polyakov SV, Fan J, Bienfang JC. Single-photon generation and detection: physics and applications, vol. 45. Cambridge, MA, USA, Academic Press, 2013.
- [74] Leuthold J, Koos C, Freude W. Nonlinear silicon photonics. *Nat Photonics* 2010;4:535–44.
- [75] Sharping JE, Lee KF, Foster MA, Turner AC, Schmidt BS, Lipson M, Gaeta AL, Kumar P. Generation of correlated photons in nanoscale silicon waveguides. *Opt Express* 2006;14:12388–93.
- [76] Takesue H, Tokura Y, Fukuda H, Tsuchizawa T, Watanabe T, Yamada K, Itabashi S-I. Entanglement generation using silicon wire waveguide. *Appl Phys Lett* 2007;91:201108.
- [77] Xiong C, Monat C, Clark AS, Grillet C, Marshall GD, Steel MJ, Li J, O’Faolain L, Krauss TF, Rarity JG, Eggleton BJ. Slow-light enhanced correlated photon pair generation in a silicon photonic crystal waveguide. *Opt Lett* 2011;36:3413–5.
- [78] Xiong C, Zhang X, Mahendra A, He J, Choi D-Y, Chae CJ, Marpaung D, Leinse A, Heideman RG, Hoekman M, Roeloffzen CGH, Oldenbeuving RM, van Dijk PWL, Taddei C, Leong PHW, Eggleton BJ. Compact and reconfigurable silicon nitride time-bin entanglement circuit. *Optica* 2015;2:724–7.
- [79] Xiong C, Collins MJ, Steel MJ, Krauss TF, Eggleton BJ, Clark AS. Photonic crystal waveguide sources of photons for quantum communication applications. *IEEE J Select Topics Quantum Electron* 2015;21:205–14.
- [80] Azzini S, Grassani D, Galli M, Andreani LC, Sorel M, Strain MJ, Helt LG, Sipe JE, Liscidini M, Bajoni D. From classical four-wave mixing to parametric fluorescence in silicon microring resonators. *Opt Lett* 2012;37:3807–9.
- [81] Azzini S, Grassani D, Galli M, Gerace D, Patrini M, Liscidini M, Velha P, Bajoni D. Stimulated and spontaneous four-wave mixing in silicon-on-insulator coupled photonic wire nano-cavities. *Appl Phys Lett* 2013;103:031117.
- [82] Davanco M, Ong JR, Shehata AB, Tosi A, Agha I, Assefa S, Xia F, Green WMJ, Mookherjee S, Srinivasan K. Telecommunications-band heralded single photons from a silicon nanophotonic chip. *Appl Phys Lett* 2012;100:261104.
- [83] Savanier M, Kumar R, Mookherjee S. Optimizing photon-pair generation electronically using a p-i-n diode incorporated in a silicon microring resonator. *Appl Phys Lett* 2015;107:131101.
- [84] Ong JR, Kumar R, Mookherjee S. Silicon microring-based wavelength converter with integrated pump and signal suppression. *Opt Lett* 2014;39:4439–41.
- [85] Matsuda N, Karkus P, Nishi H, Tsuchizawa T, Munro WJ, Takesue H, Yamada K. On-chip generation and demultiplexing of quantum correlated photons using a silicon-silica monolithic photonic integration platform. *Opt Express* 2014;22:22831–40.
- [86] Clemmen S, Phan Huy K, Bogaerts W, Baets RG, Emplit PH, Massar S. Continuous wave photon pair generation in silicon-on-insulator waveguides and ring resonators. *Opt Express* 2009;17:16558–70.
- [87] Gentry CM, Shainline JM, Wade MT, Stevens MJ, Dyer SD, Zeng X, Pavanello F, Gerrits T, Nam SW, Mirin RP, Popović MA. Quantum-correlated photon pairs generated in a commercial complementary metal-oxide semiconductor microelectronics chip. *arXiv preprint* 2015. [arXiv:1507.01121](https://arxiv.org/abs/1507.01121).
- [88] Preble SF, Fanto ML, Steidle JA, Tison CC, Howland GA, Wang Z, Alsing PM. On-chip quantum interference from a single silicon ring-resonator source. *Phys Rev Applied* 2015;4:021001.
- [89] Krauss TF. Slow light in photonic crystal waveguides. *J Phys D Appl Phys* 2007;40:2666–70.
- [90] Monat C, Ebnali-Heidari M, Grillet C, Corcoran B, Eggleton BJ, White TP, O’Faolain L, Li J, Krauss TF. Four-wave mixing in slow light engineered silicon photonic crystal waveguides. *Opt Express* 2010;18:22915–27.
- [91] Helt LG, Yang Z, Liscidini M, Sipe JE. Spontaneous four-wave mixing in microring resonators. *Opt Lett* 2010;35:3006–8.
- [92] Engin, E, Bonneau D, Natarajan CM, Clark A, Tanner MG, Hadfield RH, Dorenbos SN, Zwiller V, Ohira K, Suzuki N, Yoshida H, Iizuka N, Ezaki M, O’Brien JL, Thompson MG. Photon pair generation in a silicon micro-ring resonator with reverse bias enhancement. *Opt Express* 2013;21:27826–34.
- [93] Mower J, Englund D. Efficient generation of single and entangled photons on a silicon photonic integrated chip. *Phys Rev A* 2011;84:052326.
- [94] Francis-Jones RJA, Mosley PJ. Temporal loop multiplexing: a resource efficient scheme for multiplexed photon-pair sources, *ArXiv e-prints* 2015. [arXiv:1503.06178](https://arxiv.org/abs/1503.06178).
- [95] Pittman TB, Jacobs BC, Franson JD. Single photons on pseudodemand from stored parametric down-conversion. *Phys Rev A* 2002;66:042303.
- [96] Kaneda F, Christensen BG, Wong JJ, McCusker KT, Park HS, Kwiat PG. Time-multiplexed heralded single-photon source. *Optica* 2015;2:1010–3.
- [97] Xiong C, Zhang X, Liu Z, Collins MJ, Mahendra A, Helt LG, Steel MJ, Choi D-Y, Chae CJ, Leong PHW, Eggleton BJ, Xiong C, Zhang X,

- Liu Z, Collins MJ, Mahendra A, Helt LG, Steel MJ, Choi D-Y, Chae CJ, Leong PHW, Eggleton BJ. Active temporal multiplexing of indistinguishable heralded single photons. *Nat Commun* 2016;7. arXiv:1508.03429.
- [98] Mendoza GJ, Santagati R, Munns J, Hemsley E, Piekarek M, Martin-Lopez E, Marshall GD, Bonneau D, Thompson MG, O'Brien JL. Active temporal multiplexing of photons. 2015. arXiv:1503.01215.
- [99] Migdall AL, Branning D, Castelletto S. Tailoring single-photon and multiphoton probabilities of a single-photon on-demand source. *Phys Rev A* 2002;66:053805.
- [100] Shapiro JH, Wong FN. On-demand single-photon generation using a modular array of parametric downconverters with electro-optic polarization controls. *Opt Lett* 2007;32:2698–700.
- [101] Ma X-S, Zotter S, Kofler J, Jennewein T, Zeilinger A. Experimental generation of single photons via active multiplexing. *Phys Rev A* 2011;83:043814.
- [102] Hadfield RH. Single-photon detectors for optical quantum information applications. *Nat Photonics* 2009;3:696–705.
- [103] Marsili F, Verma VB, Stern JA, Harrington S, Lita AE, Gerrits T, Vayshenker I, Baek B, Shaw MD, Mirin RP, Nam SW. Detecting single infrared photons with 93% system efficiency. *Nat Photonics* 2013;7:210–4.
- [104] Najafi F, Dane A, Bellei F, Zhao Q, Sunter KA, McCaughan AN, Berggren KK. Fabrication process yielding saturated nanowire single-photon detectors with 24-ps jitter. *IEEE J Sel Top Quant* 2014;21:1–7.
- [105] Rosfjord KM, Yang JK, Dauber EA, Kerman AJ, Anant V, Voronov BM, Gol'tsman GN, Berggren KK. Nanowire single-photon detector with an integrated optical cavity and anti-reflection coating. *Opt Express* 2006;14:527–34.
- [106] Heeres RW, Kouwenhoven LP, Zwiller V. Quantum interference in plasmonic circuits. *Nat Nanotechnol* 2013;8:719–22.
- [107] Sahin D, Gaggero A, Hoang TB, Frucci G, Mattioli F, Leoni R, Beetz J, Lermer M, Kamp M, Höfling S, Fiore A. Integrated autocorrelator based on superconducting nanowires. *Opt Express* 2013;21:11162–70.
- [108] Pant M, Krovi H, Englund D, Guha S. Rate-distance tradeoff and resource costs for all-optical quantum repeaters. *ArXiv e-prints* 2016. arXiv:1603.01353.
- [109] Kieling K, Rudolph T, Eisert J. Percolation, renormalization, and quantum computing with nondeterministic gates. *Phys Rev Lett* 2007;99:130501.
- [110] Zaidi HA, Dawson C, van Loock P, Rudolph T. Near-deterministic creation of universal cluster states with probabilistic bell measurements and three-qubit resource states. *Phys Rev A* 2015;91:042301.
- [111] Almeida VR, Barrios CA, Panepucci RR, Lipson M. All-optical control of light on a silicon chip. *Nature* 2004;431:1081–4.